Investigation of Strength and Formability of 6016 Aluminum Tailor Welded Blanks

metals

MDPI

Article

Investigation of Strength and Formability of 6016 Aluminum Tailor Welded Blanks

Dario Basile [1], Raffaella Sesana [2], Manuela De Maddis [1], Luca Borella [3] and Pasquale Russo Spena [1,*]

[1] Department of Management and Production Engineering, Politecnico di Torino, Corso Duca degli Abruzzi 24, 10129 Turin, Italy
[2] Department of Mechanical and Aerospace Engineering, Politecnico di Torino, Corso Duca degli Abruzzi 24, 10129 Turin, Italy
[3] CO.ST.AT., Via Del Mare 19, Piobesi Torinese, 10040 Turin, Italy
* Correspondence: pasquale.russospena@polito.it; Tel.: +39-01-1090-7298

Abstract: The automotive industry is constantly looking for innovative techniques to produce lighter, more efficient, and less polluting vehicles to comply with the increasingly restrictive environmental regulations. One of the latest technologies, which is still developing, is based on the fabrication of the body-in-white and car parts through the stamping of aluminum tailor welded blanks. Tailor welded blanks (TWBs) are generally a combination of two/three metal sheets with different thicknesses and/or mechanical strengths, which are commonly laser butt-welded. Even though the aluminum TWBs have the main advantage of producing lightweight parts, their use is still limited by the lower formability than their parent materials and by the fact that laser welding of aluminum sheets still remains a process easily subjected to weld defects (i.e., internal porosity) and, hence, requires strict control of process parameters. This study has investigated the effects of the main laser welding process parameters (laser power, welding speed, and focus position) on the mechanical properties and formability of aluminum TWBs made of the 6xxx series. The research results show that the welding conditions highly influence the weldability of such alloys. Heat input over 70 J/mm is responsible for excessive porosity and molten pool (and consequent root concavity), which are responsible for the lowest mechanical strength and formability of joints. Differently, low amounts of imperfections have a limited influence on the mechanical behaviors of the TWB joints. Overall, a narrow weldability window is required to ensure welded joints with proper strength and limited or no porosity.

Keywords: tailor welded blanks; laser welding; aluminum sheets; automotive industry; mechanical properties; joint geometrical features

Citation: Basile, D.; Sesana, R.; De Maddis, M.; Borella, L.; Russo Spena, P. Investigation of Strength and Formability of 6016 Aluminum Tailor Welded Blanks. *Metals* **2022**, *12*, 1593. https://doi.org/10.3390/met12101593

Academic Editor: Jean-Michel Bergheau

Received: 30 May 2022
Accepted: 16 September 2022
Published: 24 September 2022

1. Introduction

The automotive industry is constantly looking for innovative techniques to produce lighter, more efficient, and less polluting vehicles to fulfill the increasingly restrictive environmental regulations. One of the advanced solutions to meet these requirements is the adoption of steel car parts obtained from the stamping of tailor welded blanks (TWBs). A TWB is a welded sheet commonly obtained by laser butt welding of different metal sheets (usually made of two or three steel grades) with various thicknesses and/or strengths. Then, the TWB is subjected to stamping to obtain the final parts [1]. The main advantage of TWBs lies in tailoring the mechanical strength of the automotive parts by only reinforcing, with more resistant materials, those regions that need strength or stiffness for crash resistance (such as pillars, door hinge reinforcements, and tunnels) and saving materials by maintaining a lower thickness in the rest of the component where strength is not necessary. The use of TWBs results in a reduction of the weight of the vehicle and, hence, fuel emission, and fuel consumption as well as an increase in performance [2]. The 10% decrease in the weight of vehicles leads to a reduction in fuel consumption of around 6–8%. Moreover, material, transport, and manufacturing costs can be reduced.

To stress the reduction of vehicle weight, the automotive industry is increasingly adopting aluminum alloys for the fabrication of car parts. It has been estimated that replacing steel with aluminum in body-in-white can result in weight savings as high as 55% [3]. Aluminum alloys of the 5xxx and 6xxx series are typically supplied to automotive manufacturers for the production of car body parts and door structural components. This is because of their notable properties, including proper strength, high corrosion resistance, weldability, and adequate formability [4].

There are a few studies concerning the fabrication of aluminum TWBs. Overall, the literature has shown that the mechanical properties and formability of TWBs are notably influenced by welding parameters, including joining technique, laser beam [5] and FSW [6], laser power, rotational speed of the FSW tool, welding speed, and so forth. Welding parameters especially influence heat-treatable aluminum alloys since little changes in welding settings can result in different local heat treatment conditions, weld sizes, and defects, which lead to notable changes in the local mechanical properties and formability of the welded seam and, hence, in the overall mechanical performance of TWBs [7,8]. Friedman and Kridli [3] investigated the mechanical and microstructural properties of laser-welded joints between 5xxx and 6xxx series aluminum alloys. Tensile tests showed that the joints obtained from the sheets of the same thickness failed in the weld, while in dissimilar joints, the fracture occurred in the base metal of the sheet with the lower thickness. The cause of this different behavior has been identified in welding seam geometry: in the dissimilar joints, the cross-section of the weld is larger and, hence, more resistant than the thinner sheet; while in similar joints, the weld cross-section is almost the same as that of the sheets, and so the weld fails in advance because of its lower mechanical strength. This study also pointed out that the thinner sheets underwent a much greater deformation at fracture. The limiting dome height tests showed that TWB formability depends on the orientation of the welding line, the better results were obtained as the welding line was inclined by 45° with respect to the stretch direction. Shakeri et al. [9] performed formability tests (limiting dome height) on laser and electron beam welded EN AW 5754 aluminum sheets with different thickness ratios. The welded samples failed either in the welding seam or in the base material, the position of the fracture depending on the thickness ratio and the weld orientation. Specifically, the formability of the joints decreases as the thickness ratio increases. The presence of welding defects, their type, and distribution strongly reduced formability compared to the base material, especially for low thickness ratios. Shibata et al. [10] studied the effect of laser power and welding speed on the mechanical strength and formability of twin spot laser welding of EN AW 5183 aluminum sheets, identifying an acceptable range of these process parameters. Tensile tests performed on welded samples with different thickness ratios showed that the failure only occurred in the base material with the minor thickness if the minimum thickness of the welding seam was greater than at least 10% of the sheet metal. A formability test (ball elongation test) showed that the weldment (thickness of 1 and 2 mm) exhibited a deformation 30% less than that of the base material of greater thickness. A real rear door from aluminum TWB showed a stiffness like the same component made of steel. Wang et al. [11] determined the effect of the thickness ratio on the formability of laser-welded EN AW 6082 aluminum sheets after heating (solubilization) of the TWB, quenching during the stamping process, and the final artificial aging. It has been observed that the mechanical properties of the parent metal could be restored in the weldment by this treatment. The welding line moved more from its original position (caused by the deformation) for larger thickness ratios. The results of this study were used to set up a finite element model to predict the movement of the welding line and the deformation field. Bagheri et al. [12] compared the tensile strength and formability of welded sheets of EN AW 6061 aluminum (thicknesses of 0.8–1.2 mm) obtained using three different welding methods: laser, friction stir welding (FSW), and friction stir vibrating welding (FSVW). Welded sheets obtained from FSW and FSVW exhibited greater formability, mainly due to the finer microstructure than laser welds. Jie et al. (2007) [13] also investigated the mechanical strength and formability of laser-

welded EN AW 5754 aluminum sheets (thickness 1–1.3 mm) to set up a FEM simulation capable of predicting the formability limits of welded joints. Liu et al. [14] have reported an interesting investigation on the effect of welding size with respect to specimen dimension on the evaluation of the mechanical properties of AA6082 tailor welded specimens. This work proposes a model based on plasticity theory to predict the mechanical properties of the tailor welded specimen. It was found that the yield strength increases with the increasing dimensions of the tensile specimens. The deformation behavior of the different zones of the specimens (HAZ, fusion zone, and base metals) has been assessed through the Digital Image Correlation (DIC) technique.

Miles et al. [15] used three different aluminum alloys (5182-O, 5754-O, and 6022-T4) to evaluate the strength and formability of Al TWBs, comparing TIG and FSW welding technologies to each other. Results showed that 5xxx series alloys had similar ductility and formability for both welding technologies. FSW allowed better performance on 6022-T4 AA, showing similar formability between the welded and the base material under plane-strain conditions, but formability decreased significantly in the welded joint when the biaxial strain condition approached the strain occurring across the weld.

Parente et al. [16] evaluated the formability of FSW 5182/6061 aluminum alloys, 1 mm thick, through the Nakajima test. Results showed how the weld line orientations affected the formability performances: the longitudinal TWBs exhibited the highest value for the load-displacement curves and the worst performances for transversal weld lines, while the 45° orientation displayed an intermediate behavior.

This work aims to describe the laser butt welding of 6016 aluminum alloys to produce TWBs by investigating the relationship between the main process parameters (laser power, welding speed, and focus position) and weld quality through microstructural and mechanical characterization of the welded joints. Finally, Erichsen tests have also been performed to evaluate the formability of the aluminum-based TWBs at varying welding conditions.

2. Materials and Methods

This study has been conducted on 1.2 and 2 mm thick 6016-T4 aluminum alloy sheets for automotive purposes. These alloys can be used for parts of the body panels, including fenders and hooks, due to their relatively good strength and dent resistance. The nominal chemical composition of the 6061 sheets is listed in Table 1. The experimental TWBs have been obtained by dissimilar laser butt-welding of the 6061 sheets with different thicknesses.

Table 1. Nominal chemical composition, % vol., of the 6016 aluminum alloy.

Al Alloy	Al	Mg	Si	Mn	Fe	Cr	Cu	Zn	Ti
6016	bal.	0.3–0.6	1.0–1.5	≤0.2	≤0.5	-	≤0.2	-	-

For each thickness, coupons with a size of 122 × 408 mm were extracted from the 6061 sheets. The coupons were all cut from the same sheet and along the rolling direction and cleaned with acetone to remove contaminants (e.g., oxide, oil) from the metal surfaces to limit welding defects. During each welding test, two coupons with different thicknesses were placed in a clamping system, Figure 1, and joined together by laser butt welding using a TruLaser Cell Series 7040 system with the Nd-YAG laser source TRUMPF Trudisk 4001 (maximum power of 4000 W, beam wavelength of 1.030 μm) (Trumpf, Ditzingen, Germany). The weld line was parallel to the rolling direction. The incidence angle of the laser beam was 20° with respect to the vertical direction.

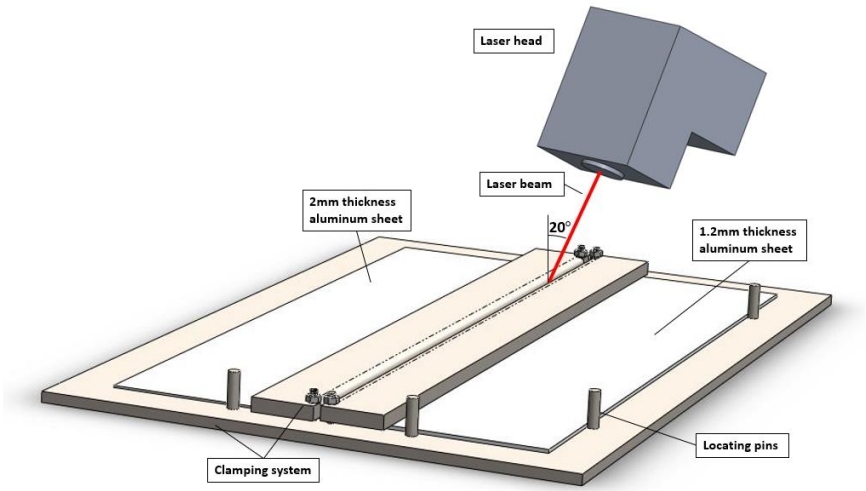

Figure 1. Mechanical fixture for welding the aluminum sheet coupons and laser welding.

The welding tests were performed at the CO.ST.AT. company (Turin, Italy) to assess the influence of the main welding process parameters such as laser power, welding speed, and focus position on the joint mechanical properties. The focus position is the distance of the laser focus from the surface of the thicker aluminum sheet. Based on preliminary experiments, the welding parameters were varied at different levels, as reported in Table 2, and were set to have a suitable range of heat input per unit of length of about 50 to 80 J/mm. The heat input was calculated as the ratio of laser power to welding speed. Since the experimental tests were performed in collaboration with a firm, the numerical values of the laser power and welding speed are reported directly (laser power as a percentage of the maximum power developed by the equipment welding speed is normalized to its lowest value).

Table 2. Nd-YAG Laser welding process parameters.

No. Run	Laser Power (%)	Welding Speed (-)	Focus Position (mm)	Heat Input (J/mm)
1	62.5	1.25	1.5	60
2	62.5	1	1	75
3	62.5	1.5	2	50
4	67.5	1.25	2	64
5	67.5	1	1.5	81
6	67.5	1.5	1	54

Welded specimens were extracted from the welded coupons through water jet cutting to perform tensile and Erichsen tests to determine tensile strength and formability at varying welding conditions. Other samples were extracted for metallographic examination. The water jet cutting process has been chosen as it provides an excellent surface finish and does not thermally alter the microstructure of the joints in accordance with the requirements of the ISO 4136 standard [17]. The sampling scheme with the specimen sizes for the microstructural examination and mechanical tests is displayed in Figure 2.

An Instron8801 servo-hydraulic machine (Instron, Norwood, MA, USA) 100 kN load cell, 12.5 mm gauge length extensometer, has been used to perform the tensile test based on the ISO 4136 standard [17]. The Erichsen tests were carried out according to the ISO 20482 standard [18] on the same servo-hydraulic machine by means of dedicated testing equipment. For each setting parameter in Table 2, three tensile and formability tests were performed to have consistent results.

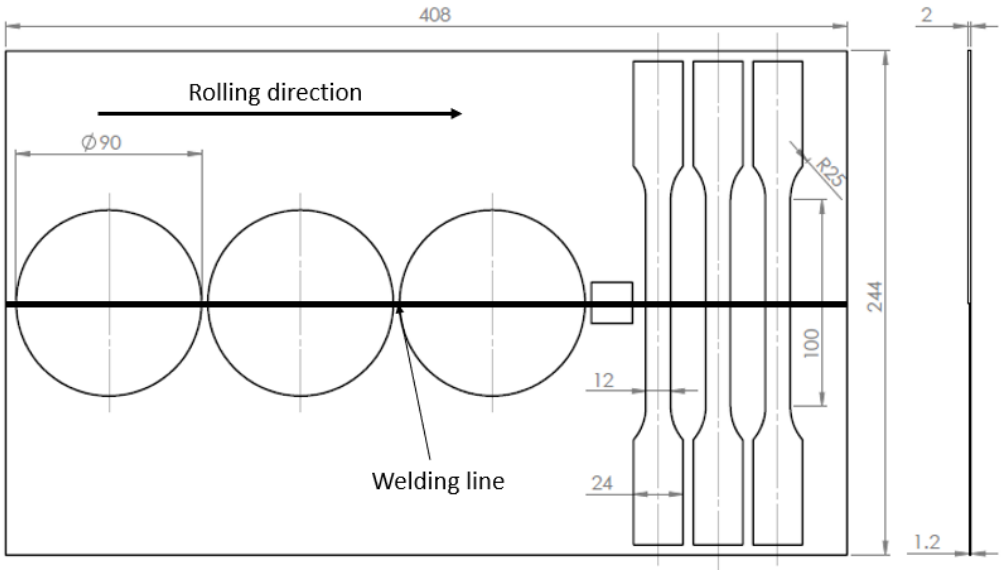

Figure 2. Sampling scheme of the specimens used in the metallographic examination and mechanical (tensile and Erichsen) tests.

The metallographic samples were subjected to a standard examination through a preliminary grounding and polishing, followed by a final chemical etching with Keller reagent (95 mL water, 2.5 mL HNO_3, 1.5 mL HCl, 1.0 mL HF). The cross-section of the welded joint microstructures and the parent metals have been examined with an optical microscope (Zeiss Axiovert, Oberkochen, DE).

3. Results

3.1. Metallographic Examination

Figure 3 shows the typical weld bead shape and microstructures of an Al laser butt joint. The joint microstructures change according to the heat input involved during the welding process. In the fusion zone (FZ), the joints exhibit a coarse α-phase microstructure coherently with the solidification of the weld pool. Grains are also coarse in the heat affected zone (HAZ) next to the FZ. In that region, the α-phase grains have an average size of about 20–25 µm. Moving away from the FZ, the grain size of the HAZ reduces continuously toward the base material, where the grain size is about 5 µm. The HAZ region is quite narrow, about 0.5–1 mm.

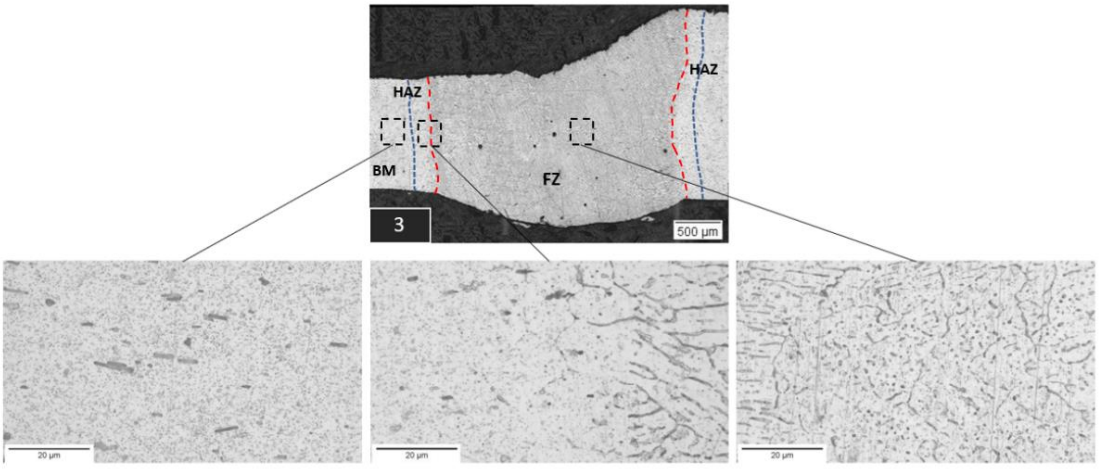

Figure 3. Typical metallographic cross-section of the welded joints and microstructure of the fusion zone, HAZ, and base material.

The geometrical shape of the welded joints has been evaluated according to the ISO 13919-2 standard [19]. This standard gives the requirements and recommendations on quality levels for imperfections of aluminum laser welded joints. The shape imperfections of the laser welded joints have been evaluated, such as root penetration and root concavity, as shown in Figure 4a, and misalignment of the sheets, as shown in Figure 4b.

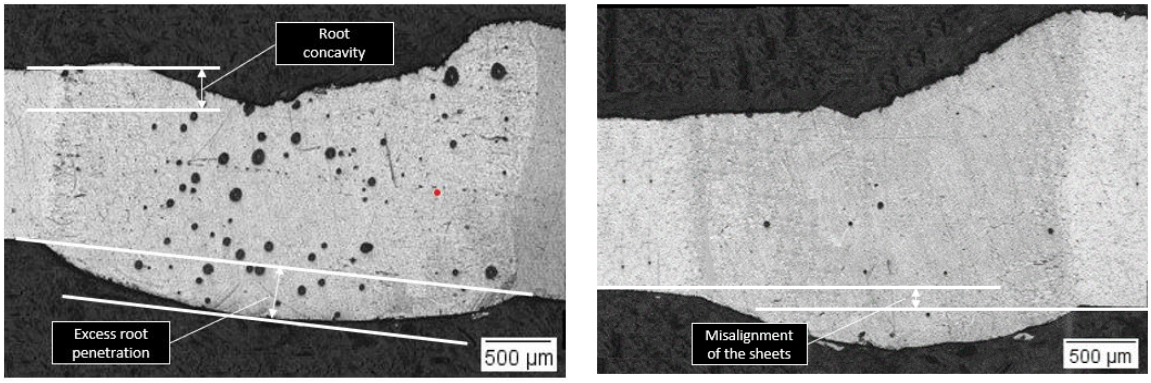

(**a**) (**b**)

Figure 4. Welded joint imperfections according to the ISO 13919-2 standard: (**a**) root concavity and excess root penetration; (**b**) misalignment of the sheets.

Figure 5 shows the influence of process parameters on the size and shape of the weld beads. As shown in Table 2, the welding settings involve different heat inputs, which influence the resulting joints. The focus position determines the area on the sheets covered by the laser beam and, hence, the power density (i.e., the ratio of the laser power and the beam spot area).

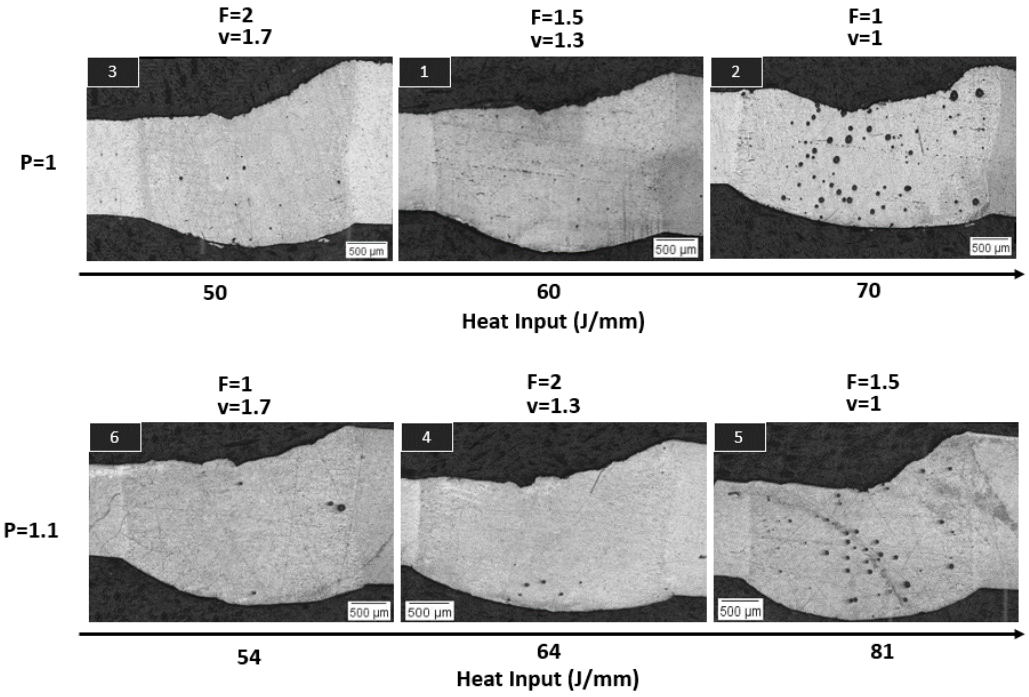

Figure 5. Cross-sections of the welded joints at varying welding conditions. P: laser power (normalized value); v: welding speed (normalized value); F: focus position (mm).

The size of the weld bead imperfections (refer to Figure 5) has been reported in Table 3. All the specimens have a misalignment defect. Specimens no. 2, 4, and 6 have the largest misalignment. As expected, the excess root penetration increases with the laser power

according to the heat input developed during the joining process. Specimens 2, 4, and 5 also have a concavity defect. In particular, specimen 2 has the largest root concavity.

Table 3. Geometrical imperfections of the welded joints at varying welding conditions. W_t: weld width at the top surface; D_f: depth of the fusion zone.

No. Run	Sheet Misalignment (mm)	Excess Root Penetration (mm)	Root Concavity (mm)	Aspect Ratio, W_t/D_f (-)
1	0.29	0.40	0	1.66
2	0.46	0.39	0.27	2.26
3	0.13	0.35	0	1.67
4	0.42	0.44	0.12	1.72
5	0.16	0.47	0.13	1.92
6	0.40	0.51	0	1.71

Almost all the welded joints show some porosity defects. Samples no. 2 and 5 have the larger number of pores inside the weld bead, coherently with the maximum heat inputs. Other studies have also found how aluminum weldments are normally affected by porosity, with voids that may be more or less prevalent according to the welding parameters and practice [20–22]. Low welding speed and positive defocus increase the peak temperatures of the weld zone, thus promoting the formation of porosity [23]. Kim et al. [24] also have found that the effect of the defocus value on the porosity formation rate is particularly evident for AA6061 alloys because of the presence of light elements such as Mg and Zn. According to Kutsuna et al. [25], the main causes of porosity in aluminum alloys are the vaporization of the low-melting alloying elements and surface contamination (including hydrogen in the surface oxide layer). However, by measuring the size of the pores and calculating the density of porosity in the joint surface, it was found that all welded joints comply with standard ISO 13919-2 [19].

Table 3 also reports the average aspect ratio of the welded beads. The aspect ratio has been measured as the ratio of the weld width at the top surface (W_t) to the depth of the fusion zone (D_f). All the joints have an aspect ratio of over 1.6. The highest values of the aspect ratio have been found for specimens 2 and 5, which are the specimens with the worst porosity. This result agrees with the study of Sun et al. [23]. They found that the porosity in welded aluminum sheets increases when the aspect ratio increases, which corresponds with a reduction in the weld depth and an increase in the weld width, thus leading to a reduction in the peak temperature.

3.2. Tensile Test

Figure 6 shows the results of the tensile tests performed on the aluminum base material and laser-welded samples. The tests on the base material were only run on the 2 mm thick specimen since, as demonstrated by other studies [26], the sheet thickness for thin laminates does not influence the results of the mechanical tests of aluminum alloys. The welded joints failed either in the base metal or in the joints. When the welded samples failed in the joints, the fracture occurred in the fusion zone close to the interface with the HAZ of the thinner aluminum sheet. This is because the joint has the smallest cross-section in this region (see Figure 5). These results are coherent with the study of Friedman and Kridli [3] on dissimilar welding of 5xxx and 6xxx series aluminum alloys. They also found that the welding seam geometry influenced the fracture of the dissimilar joints, with the smaller cross-section of the joints failing in advance, basically because of their smaller resistance. For this reason, the engineering stress for the welded joints has been computed considering a cross-section area like that of the thinner sheet (1.2 mm).

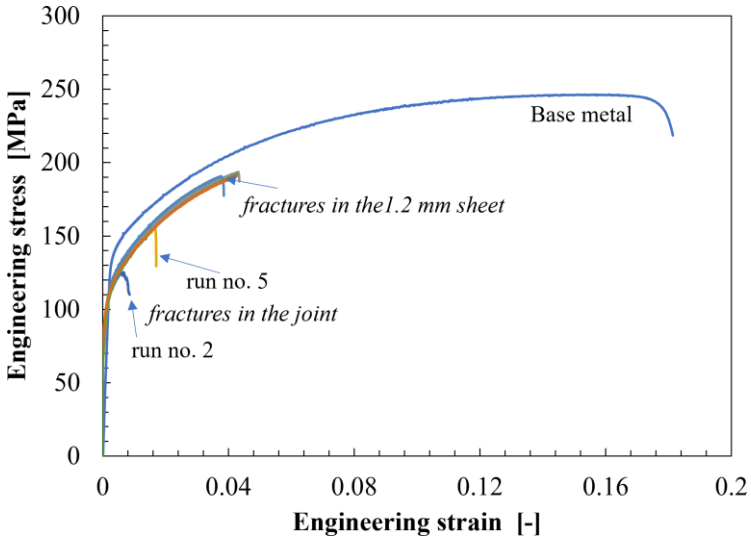

Figure 6. Engineering stress-strain curves for the 2 mm thick base metals and the welded joints.

The welded specimens exhibit a lower mechanical strength than the base metal (for the strongest welded samples, about 190 vs. 240 MPa), with a clear reduction in fracture elongation (for the strongest welded samples, 5% vs. 19%). This is primarily due to the improper coarse microstructure of the joints, which is generally known to have lower ductility than the base materials. As expected, the welded joints with the larger amount of porosity (runs no. 2 and 5 in Figure 5) fractured in the weld seam with the worst mechanical performance. These results agree with the literature. Some studies have pointed out a clear reduction in the mechanical strength of TWB specimens with respect to the base material for 6082 [14] and 7075 alloys [27]. Venkat et al. [21] reported that welds of 6111 alloys achieved one-third of the elongation of the parent metal. The welded specimens that failed in the thin sheet exhibit the highest mechanical strength and elongation at fracture with a clear necking at the fracture surface, Figure 7. In this case, the thinner sheet elongated more than the thicker aluminum sheet due to the dissimilar thickness of the welded samples. Specimen no. 2 exhibits lower mechanical strength and ductility with respect to specimen no. 5. The reason could be that, even though both the specimens have a higher amount of porosity, specimen no. 2 also shows a larger root concavity, which would promote a premature failure of the weld.

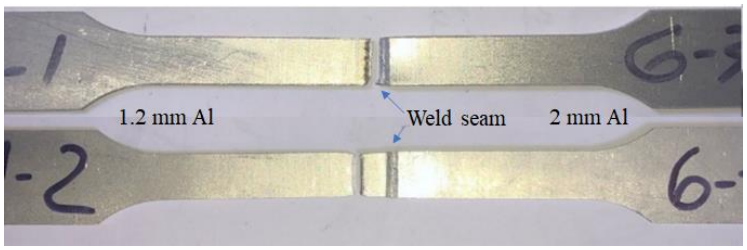

Figure 7. Examples of welded samples fractured in the welded joints (top sample) and the 1.2 mm thick aluminum sheet (bottom sample).

Tensile test results are also reported in Figure 8 as a function of the heat input to evaluate its effect on the mechanical properties of the welded joints. It can be seen that excessive heat inputs have a harmful effect on the joint strength, as previously discussed, due to the porosity and root concavity (samples no. 2 and 5). Therefore, a heat input of less than about 70 J/mm should be used to obtain sound joints for the examined Al sheets. The joints welded with such heat input (runs no. 1, 3, 4, and 6) have a similar tensile load, being the mechanical resistance of the weld bead.

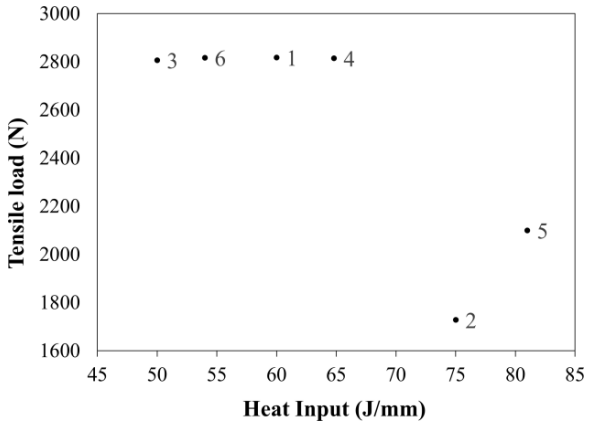

Figure 8. Maximum tensile load of the welded joints versus heat input. The numbers in the graph refer to the experimental run.

3.3. Erichsen Test

Although the chemical composition of the aluminum alloys used for TWBs is of major interest, the ductility of the weld seam also has a key role since it influences the survival of the TWB during the stamping operation. Figure 9 shows the load-displacement curves obtained from the formability test performed on the TWB coupons. The Erichsen Index can be computed from the curves as the displacement of the punch at the peak load where the specimen experienced the fracture. The test confirms the lower ductility of the welded joints than the base metals. The Erichsen index is about 3.5–3.7 mm for the more ductile welded joints vs. an index of 7 mm measured for the 2 mm thick aluminum sheet.

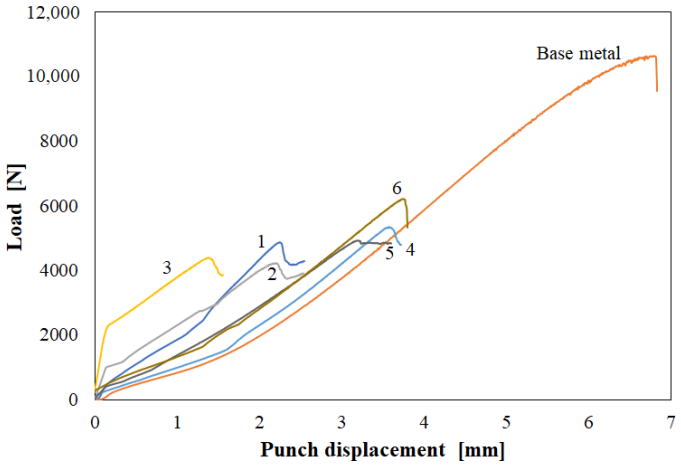

Figure 9. Load-punch displacement curves of the Erichsen cupping tests of the welded joints (the numbers in the graph refer to the experimental runs) and the 2 mm thick base metal.

As shown in Figure 10, the rupture occurred in the weld seam for all the specimens, with the crack that nucleated in the weld seam and then propagated through the welding line. The maximum value of standard deviation (based on three replications) has been obtained for specimen no. 2, which has the larger amount of porosity. The voids have the effect of generating strain gradients in the weld seam when under external loading. This feature makes the weld formability driven by an uneven strain field throughout the weld seam. Friedman and Kridli [3] also found the same results, with the crack propagating through the less resistant and more brittle weld seam with respect to the base materials. The larger grain size in the weld regions could have contributed to further reducing the capability of the joints to withstand the stretching load. Similar trends in the Erichsen diagram and failure mode of the TWB samples have also been reported in other studies

that used friction stir welded tailor blanks to fabricate TWBs made of Al 5182, 5754, and 6022 alloys [15,16].

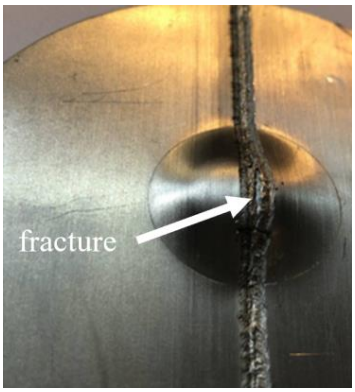

Figure 10. Example of fracture in the weld seam of an Erichsen cupping test specimen.

4. Conclusions

This study has investigated the effects of the main laser welding process parameters (laser power, welding speed, and focus position) on the mechanical properties and formability of aluminum TWBs made of the Al 6xxx series. The following conclusions can be drawn:

- The largest heat inputs (from 75 J/mm) generate welded joints with large porosity. The porosity has a clear effect on reducing the strength of the joints. Moreover, the largest root concavity and joint aspect ratio have been obtained at these heat input levels.
- Under the tensile test, the joints fracture in the thinner base metals with the smallest cross-sectional area when they show a low amount of porosity.
- The more resistant joints exhibit a tensile strength of around 190 MPa vs. 240 MPa of the base metals. The elongation at fracture of the welded joints is notably lower than the base metal (5% vs. 19%). This difference is mainly due to the dissimilar thickness of the welded samples, with the thinner sheet that elongates more than the thicker aluminum sheet.
- The Erichsen index is about 3.5–3.7 mm for the more ductile welded joints vs. an index of 7 mm measured for the 2 mm thick aluminum sheet.

Overall, the examined dissimilar joints made of 1.2 and 2 mm thick 6016 Al sheets show adequate mechanical strength and formability if proper heat inputs are adopted during welding. However, the weldability of such alloys is highly influenced by the welding conditions. Narrow weldability windows are required to limit the occurrence of porosity in the welded joints and, hence, to ensure adequate mechanical performance after the joining process. All TWBs should be designed for automotive parts that should not experience a significant degree of stretching during the forming operations.

Author Contributions: Conceptualization, D.B. and R.S.; Data curation, D.B. and R.S.; Investigation, D.B., M.D.M. and P.R.S.; Methodology, R.S.; Resources, L.B.; Supervision, R.S., M.D.M. and P.R.S.; Writing—original draft, D.B., M.D.M. and P.R.S.; Writing—review & editing, P.R.S. All authors have read and agreed to the published version of the manuscript.

Funding: This research received no external funding.

Institutional Review Board Statement: Not applicable.

Informed Consent Statement: Not applicable.

Data Availability Statement: Not applicable.

Acknowledgments: The authors are grateful to the firm *CO.ST.AT.* (Piobesi Torinese, Turin, Italy) for providing the technical support, materials, and equipment for the welding tests.

Conflicts of Interest: The authors declare no conflict of interest.

References

1. Peister, C.; George, L.; Omer, K.; Worswick, M.J.; Malcolm, S.; Dykeman, J.; Yau, C.; Soldaat, R.; Bernert, W. Forming of an axially tailored automotive channel section through hot stamping of tailor-welded blanks. *J. Phys. Conf. Ser.* **2017**, *896*, 012052. [CrossRef]
2. Merklein, M.; Johannes, M.; Lechner, M.; Kuppert, A. A review on tailored blanks—Production, applications and evaluation. *J. Mater. Proc. Technol.* **2014**, *214*, 151–164. [CrossRef]
3. Friedman, P.A.; Kridli, G.T. Microstructural and mechanical investigation of aluminum tailor-welded blanks. *J. Mater. Eng. Perform.* **2000**, *9*, 541–551. [CrossRef]
4. Snopiński, P.; Tański, T.; Gołombek, K.; Rusz, S.; Hilser, O.; Donič, T.; Nuckowski, P.M.; Benedyk, M. Strengthening of AA5754 Aluminum Alloy by DRECE Process Followed by Annealing Response Investigation. *Materials* **2020**, *13*, 301. [CrossRef] [PubMed]
5. Cao, X.; Wallace, W.; Poon, C.; Immarigeon, J.P. Research and progress in laser welding of wrought aluminum alloys. I. Laser welding processes. *Mater. Manuf. Proc.* **2003**, *18*, 1–22. [CrossRef]
6. Liu, H.J.; Fujii, H.; Maeda, M.; Nogi, K. Tensile properties and fracture locations of friction-stir-welded joints of 2017-T351 aluminum alloy. *J. Mater. Proc. Technol.* **2003**, *142*, 692–696. [CrossRef]
7. Aydın, H.; Bayram, A.; Uguz, A.; Akay, K.S. Tensile properties of friction stir welded joints of 2024 aluminum alloys in different heat-treated-state. *Mater. Des.* **2009**, *30*, 2211–2221. [CrossRef]
8. Zadpoor, A.A.; Sinke, J.; Benedictus, R. Mechanics of tailor welded blanks: An overview. *Key Eng. Mater.* **2007**, *344*, 373–382. [CrossRef]
9. Shakeri, H.R.; Buste, A.; Worswick, M.J.; Clarke, J.A.; Feng, F.; Jain, M.; Finn, M. Study of damage initiation and fracture in aluminum tailor welded blanks made via different welding techniques. *J. Light Met.* **2002**, *2*, 95–110. [CrossRef]
10. Shibata, K.; Iwase, T.; Sakamoto, H.; Kasukawa, M.; Chiba, K.; Saeki, H. Welding of aluminium tailored blanks by Nd: YAG lasers. *Weld. Int.* **2003**, *17*, 282–286. [CrossRef]
11. Wang, A.; Liu, J.; Gao, H.; Wang, L.; Masen, M. Hot stamping of AA6082 tailor welded blanks: Experiments and knowledge-based cloud—Finite element (KBC-FE) simulation. *J. Mater. Proc. Technol.* **2017**, *250*, 228–238. [CrossRef]
12. Bagheri, B.; Abbasi, M.; Hamzeloo, R. Comparison of different welding methods on mechanical properties and formability behaviors of tailor welded blanks (TWB) made from AA6061 alloys. *J. Mech. Eng. Sci.* **2021**, *235*, 2225–2237. [CrossRef]
13. Jie, M.; Cheng, C.; Chan, L.; Tang, C. Experimental and theoretical analysis on formability of aluminum tailor-welded blanks. *J. Eng. Mater. Technol.* **2006**, *129*, 151–158. [CrossRef]
14. Liu, J.; Wang, L.L.; Lee, J.; Chen, R.; El Fakir, O.; Chen, L.; Lin, J.; Dean, T.A. Size-dependent mechanical properties in AA6082 tailor welded specimens. *J. Mater. Proc. Technol.* **2015**, *224*, 169–180. [CrossRef]
15. Miles, M.P.; Decker, B.J.; Nelson, T.W. Formability and strength of friction-stir welded Aluminum sheets. *Metall. Mater. Trans. A* **2004**, *35*, 3461–3468. [CrossRef]
16. Parente, M.; Safdarian, R.; Santos, A.D.; Lourerio, A.; Vilaca, P.; Natal Jorge, R.M. A study on the formability of aluminum tailor welded blanks produced by friction stir welding. *Int. J. Adv. Manuf. Technol.* **2016**, *83*, 2129–2141. [CrossRef]
17. *ISO 4136:2022*; Destructive Tests on Welds in Metallic Materials—Transverse Tensile Test. International Standard of Organization (ISO): Geneva, Switzerland, 2022.
18. *ISO 20482:2013*; Metallic Materials—Sheet and Strip Erichsen Cupping Test. International Standard of Organization (ISO): Geneva, Switzerland, 2013.
19. *ISO 13919-2*; Electron and Laser-beam Welded Joints—Requirements and Recommendations on Quality Levels for Imperfections—Part 2: Aluminium, Magnesium and Their Alloys and Pure Copper. International Standard of Organization (ISO): Geneva, Switzerland, 2021.
20. Story, J.M.; Heinemann, S.; Naefeler, S. Forming and joining issues and processes for aluminum tailor welded blank application. *Light Metal Age* **1998**, *56*, 40–47.
21. Venkat, S.; Albrigth, C.E.; Ramasamy, S.; Hurley, J.P. CO_2 laser beam welding of aluminum 5754-O and 6111-T4 alloys. *Weld. J.* **1997**, *76*, 275s–282s.
22. Stasik, M.C.; Wagoner, R.H. *Aluminum and Magnesium for Automotive Applications*; Bryant, J.D., Ed.; TMS: Warrendale, PA, USA, 1996; pp. 69–83.
23. Sun, T.; Franciosa, P.; Ceglarek, D. Effect of focal position offset on joint integrity of AA1050 battery busbar assembly during remote laser welding. *J. Mater. Res. Technol.* **2021**, *14*, 2715–2726. [CrossRef]
24. Kim, J.S.; Watanabe, T.; Yoshida, Y. Effect of the beam-defocusing characteristics on porosity formation in laser welding. *J. Mater. Sci. Lett.* **1995**, *14*, 1624–1626. [CrossRef]
25. Kutsuna, M.; Yan, Q. Study on porosity formation in laser welds of aluminium alloys. *Weld. Int.* **2010**, *13*, 597–611. [CrossRef]
26. Suh, C.H.; Jung, Y.C.; Kim, Y.S. Effects of thickness and surface roughness on mechanical properties of aluminium sheets. *J. Mech. Sci. Technol.* **2010**, *24*, 2091–2098. [CrossRef]
27. Deepika, D.; Lakshmi, A.A.; Rao, C.S.; Sateesh, N.; Nookaraju, B.C.; Subbiah, R. Formability of tailor welded blanks of aluminium alloy and steel—A review. *Mater. Today* **2021**, *46*, 722–728. [CrossRef]